Informes Técnicos Ciemat 870
febrero, 1999

Anomalous Couplings in the $e^+e^- \to ZZ$ Process

J. Alcaraz (CIEMAT)
M. A. Falagán (CIEMAT)
E. Sánchez (CERN)

Departamento de Fusión y Partículas Elementales

Toda correspondenica en relación con este trabajo debe dirigirse al Servicio de Información y Documentación, Centro de Investigaciones Energéticas, Medioambientales y Tecnológicas, Ciudad Universitaria, 28040-MADRID, ESPAÑA.

Las solicitudes de ejemplares deben dirigirse a este mismo Servicio.

Los descriptores se han seleccionado del Thesauro del DOE para describir las materias que contiene este informe con vistas a su recuperación. La catalogación se ha hecho utilizando el documento DOE/TIC-4602 (Rev. 1) Descriptive Cataloguing On-Line, y la clasificación de acuerdo con el documento DOE/TIC.4584-R7 Subject Categories and Scope publicados por el Office of Scientific and Technical Information del Departamento de Energía de los Estdos Unidos.

Depósito Legal: M -14226-1995
ISSN: 1135 - 9430
NIPO: 238-99-003-5

Editorial CIEMAT

CLASIFICACIÓN DOE Y DESCRIPTORES

662000

HIGH ENERGY PHYSICS; ELECTRON-POSITRON COLLISIONS; Z* BARIONS; FERMI INTERACTIONS; ANOMALOUS DIMENSION; COUPLING

Anomalous Coupling in the $e^+e^- \to ZZ$ Process

Alcaraz,J. (CIEMAT); Falagán, M. A. (CIEMAT); Sánchez, E. (CERN)

25 pp. 12 figs. 9 refs.

Abstract:

We discuss experimental aspects related to the possible existence of anomalous ZZV couplings (V= Z, γ) in the $e^+e^- \to ZZ$ process. We find that, among several options, the optimal procedure to quantify their presence requires the inclusion of anomalous couplings in a complete four-fermion final-state generator. Various comparisons and checks proof the correctness of our calculations at the percent level.

Acoplos Anómalos en el Proceso $e^+e^- \to ZZ$

Alcaraz,J. (CIEMAT); Falagán, M. A. (CIEMAT); Sánchez, E. (CERN)

25 pp. 12 figs. 9 refs.

Resumen:

Discutimos aspectos experimentales relacionados con la posible existencia de acoplos anómalos ZZV (V= Z, γ) en el proceso $e^+e^- \to ZZ$. Encontramos que, entre varias opciones, el procedimiento óptimo para cuantificar su presencia requiere la inclusión de acoplos anómalos en un generador completo de cuaatro fermiones en el estado final. Varias comparaciones y comprobaciones prueban que nuestros cálculos son correctos al nivel del 1%.

CIEMAT Report 870
November 27, 1998

Anomalous Couplings in the $e^+e^- \to ZZ$ Process

J. Alcaraz[1], M.A. Falagán[1], E. Sánchez[2]

Abstract

We discuss experimental aspects related to the possible existence of anomalous ZZV couplings (V= Z, γ) in the $e^+e^- \to ZZ$ process. We find that, among several options, the optimal procedure to quantify their presence requires the inclusion of anomalous couplings in a complete four-fermion final-state generator. Various comparisons and checks proof the correctness of our calculations at the percent level.

To be submitted to Phys. Rev. D

---

[1]CIEMAT, Madrid, Spain (partially supported by CICYT Grant: AEN96-1645).
[2]CERN, Geneva, Switzerland.

1 Introduction

Pair production of Z bosons is one of the new processes to be studied at LEP2. Although it is a process with a rather low cross section ($\sigma_{ZZ} \approx \sigma_{WW}/20$) and experimentally difficult to observe (large and almost irreducible backgrounds), LEP2 gives the first opportunity to perform a measurement and to look for deviations from the Standard Model (SM). The study of triple-gauge boson couplings is one of the key issues at present and future colliders. No experimental limits exist yet on the possible existence of an anomalous ZZZ coupling.

This report describes the calculations and fitting procedures developed in the search for anomalous couplings. The method is currently being applied in the analysis of $e^+e^- \to f\bar{f}f'\bar{f}'$ final states by the L3 Collaboration [1].

2 Standard Model amplitude for the $e^+e^- \to ZZ$ process

The diagrams contributing at first order to the process $e^+e^- \to ZZ$ in the Standard Model are shown in Figure 1. We will assume a collision in the center-of-mass system with total energy $\sqrt{s}$. The following notation is used:

- Electron four-momentum k and helicity σ:
  - $k = (\frac{\sqrt{s}}{2}, \frac{\sqrt{s}}{2}\,\hat{e}_z)$
  - $\sigma \in \{-1, 1\}$
- Positron four-momentum $\overline{k}$ and helicity $\overline{\sigma}$:
  - $\overline{k} = (\frac{\sqrt{s}}{2}, -\frac{\sqrt{s}}{2}\,\hat{e}_z)$
  - $\overline{\sigma} \in \{-1, 1\}$
- Z four-momentum q_Z and polarization ϵ_Z:
  - $q_Z = (E, \sqrt{E^2 - M_Z^2}\,\hat{q})$; $\qquad E = \frac{\sqrt{s}}{2} + \frac{M_Z^2 - M_{Z'}^2}{2\sqrt{s}}$
  - $\epsilon_Z \equiv \epsilon_Z(\lambda_Z)$; $\qquad \lambda_Z \in \{1, 2, 3\}$
- Z four-momentum $q_{Z'}$ and polarization $\epsilon_{Z'}$:
  - $q_{Z'} = (E', -\sqrt{E'^2 - M_{Z'}^2}\,\hat{q})$; $\qquad E' = \frac{\sqrt{s}}{2} + \frac{M_{Z'}^2 - M_Z^2}{2\sqrt{s}}$
  - $\epsilon_{Z'} \equiv \epsilon_{Z'}(\lambda_{Z'})$; $\qquad \lambda_{Z'} \in \{1, 2, 3\}$

where the electron is assumed to collide along the +z axis ($\hat{e}_z$), and the Z -with mass M_Z- goes along the direction given by $\hat{q} = (\sin\theta_Z \cos\phi_Z, \sin\theta_Z \sin\phi_Z, \cos\theta_Z)$. The masses M_Z and $M_{Z'}$ are not assumed to be equal to the on-shell mass m_Z because in the following they will be consider as virtual particles decaying into fermions.

The matrix element for the $e^+e^- \to ZZ$ reaction is determined with the same method followed in [2]. It reads:

$$M_{ZZ} = -(g_\sigma^{Ze^+e^-})^2 \sqrt{s}\,\delta_{\sigma,-\overline{\sigma}} \left[\frac{S(\overline{k}, \epsilon_{Z'}^*, k - q_Z, \epsilon_Z^*, k)_{\sigma\sigma}^{\sigma}}{-2(kq_Z) + M_Z^2} + \frac{S(\overline{k}, \epsilon_Z^*, k - q_{Z'}, \epsilon_{Z'}^*, k)_{\sigma\sigma}^{\sigma}}{-2(kq_{Z'}) + M_{Z'}^2} \right] \qquad (1)$$

where the function $S(\overline{k}, \epsilon_a, k - q_b, \epsilon_b, k)^{\sigma}_{\sigma\sigma}$ is defined for instance in [3]. The left/right effective couplings of fermions to neutral gauge bosons are given by:

$$g_{+}^{\mathrm{Z}\mathrm{f}\bar{\mathrm{f}}} = -2Q_{\mathrm{f}} \sin^2\overline{\theta}_{\mathrm{W}} \left(\sqrt{2}G_{\mu}m_{\mathrm{Z}}^2\right)^{1/2} \quad (2)$$

$$g_{-}^{\mathrm{Z}\mathrm{f}\bar{\mathrm{f}}} = g_{+}^{\mathrm{Z}\mathrm{f}\bar{\mathrm{f}}} + 2\mathrm{I}_3 \left(\sqrt{2}G_{\mu}m_{\mathrm{Z}}^2\right)^{1/2} \quad (3)$$

$$g_{+}^{\gamma\mathrm{f}\bar{\mathrm{f}}} = Q_{\mathrm{f}} \left(4\pi\alpha(M_{\gamma^*}^2)\right)^{1/2} \quad (4)$$

$$g_{-}^{\gamma\mathrm{f}\bar{\mathrm{f}}} = g_{+}^{\gamma\mathrm{f}\bar{\mathrm{f}}} \quad (5)$$

where Q_{f} is the charge of the fermion f in units of the charge of the positron, and the electromagnetic coupling constant $\alpha(M_{\gamma^*}^2)$ is evaluated at the scale of the virtual photon mass $M_{\gamma^*}^2$. I_3 is the third component of the weak isospin ($\pm 1/2$), $\sin^2\overline{\theta}_{\mathrm{W}}$ is the effective value of the square of the sine of the Weinberg angle and G_{μ} is the value of the Fermi coupling constant. The effective couplings to the Z absorb the relevant electroweak radiative corrections at the scale of the Z. They are obtained by the substitutions:

$$\sin^2\theta_{\mathrm{W}} \rightarrow \sin^2\overline{\theta}_{\mathrm{W}} \quad (6)$$

$$\frac{e^2}{4\sin^2\theta_{\mathrm{W}}\cos^2\theta_{\mathrm{W}}} \rightarrow \sqrt{2}G_{\mu}m_{\mathrm{Z}}^2 \quad (7)$$

The experimental signature of a $\mathrm{e}^+\mathrm{e}^- \rightarrow \mathrm{ZZ}$ process is a final state with four fermions, due to the unstability of the Z particle. A distinctive feature is that the invariant masses of the two pairs, $\mathrm{f}\bar{\mathrm{f}}$ and $\mathrm{f}'\bar{\mathrm{f}}'$, are close to the Z mass m_{Z}. The angular distribution of the decay products keeps information on the average polarization of the Z boson. In addition, the Z decay amplitude needs to be considered for a correct treatment of spin correlations. Assuming that fermion masses are negligible compared to m_{Z}, this amplitude is given by:

$$M_{\mathrm{Z}\mathrm{f}\bar{\mathrm{f}}} = g_{\lambda}^{Zff}\, 2\sqrt{p_0\overline{p_0}}\, \delta_{\lambda,-\overline{\lambda}}\, S(p, \epsilon_{\mathrm{Z}}, \overline{p})^{\lambda}_{\lambda\lambda} \quad (8)$$

where $p, \overline{p}$ are the four-momenta of fermion and antifermion, respectively, $\lambda, \overline{\lambda}$ their helicities, and the function $S(p, \epsilon_{\mathrm{Z}}, \overline{p})$ is defined in [3].

3 Anomalous couplings in the $\mathrm{e}^+\mathrm{e}^- \rightarrow$ ZZ process

Anomalous couplings arise from interactions of the type shown in Figure 2. The coupling $\mathrm{ZZ}V$, with $V = \mathrm{Z}$ or γ, does not exist in the Standard Model at the tree level. Assuming on-shell production of Z bosons, the most general expression for the anomalous vertex function is [2]:

$$\Gamma_{\mathrm{ZZ}V}^{\alpha\beta\mu} = \frac{s - m_V^2}{m_{\mathrm{Z}}^2} \{ \;\; i\, f_4^V \left((k+\overline{k})^{\alpha}\, g^{\mu\beta} + (k+\overline{k})^{\beta}\, g^{\mu\alpha}\right) \; + \; i\, f_5^V\, \epsilon^{\alpha\beta\mu\rho}\, (q_{\mathrm{Z}\rho} - q_{\mathrm{Z}'\rho}) \; \} \quad (9)$$

A non-zero value of f_4^V leads to a C-violating,CP-violating process, while terms associated to f_5^V are P-violating, CP-conserving. Using again the formalism followed in [2] we obtain the explicit expressions for the different anomalous contributions:

$$M_{AC}^{f_4^V} = \quad -i\, e f_4^V g_\sigma^{Vee} \frac{s}{m_Z^2} \delta_{\sigma,-\bar{\sigma}} [\epsilon_Z^{0*}(\epsilon_{Z'}^{1*} + i\sigma\epsilon_{Z'}^{2*}) + \epsilon_{Z'}^{0*}(\epsilon_Z^{1*} + i\sigma\epsilon_Z^{2*})] \tag{10}$$

$$M_{AC}^{f_5^V} = \quad -i\, e f_5^V g_\sigma^{Vee} \frac{\sqrt{s}}{m_Z^2} \delta_{\sigma,-\bar{\sigma}} (\epsilon^{1\alpha\beta\rho} + i\sigma\epsilon^{2\alpha\beta\rho})\, \epsilon_{Z\alpha}^*\, \epsilon_{Z'\beta}^*\, (q_{Z\rho} - q_{Z'\rho}) \tag{11}$$

Note that no $(s - m_V^2)$ factors are present in the final expressions. Compared to the SM amplitude all anomalous contributions increase with the center-of-mass energy of the collision. We want to bring the attention to the fact that these anomalous $ZZ\gamma$ couplings are different from those considered in the $e^+e^- \to Z\,\gamma$ anomalous process [2]. Therefore, not only the anomalous ZZZ couplings, but all four anomalous parameters remain experimentally unconstrained at present.

Anomalous ZZV couplings manifest in three ways:

- A change in the observed total cross section $e^+e^- \to ZZ$.
- A modification of the angular distribution of the Z.
- A change in the average polarization of the Z bosons.

Polar angle distributions of the $e^+e^- \to ZZ$ process at $\sqrt{s} = 190$ GeV are shown in Figures 3 and 4. The Standard Model prediction corresponds to 10000 generated events. The distributions in the presence of anomalous couplings are determined for the values $f_i^V = 3; i = 4, 5; V = Z, \gamma$. Both standard and anomalous histograms are normalized to the same integrated luminosity.

Both CP-violating and P-violating couplings are found to produce a global enhancement in the number of events, with moderate changes in the angular shape. The enhancement is always stronger at low polar angles.

Finally, anomalous couplings change the average polarization of the Z, as observed in Figures 5 and 6. Note the enhancement of events for the configuration in which the Z have different polarization states in the presence of CP-violating couplings.

4 Reweighting procedure

Let us consider a set of events generated according to the Standard Model differential cross section. New distributions taking into account the anomalous couplings are obtained when every event is reweighted by the factor:

$$W'^{ZZ}(\sigma, \lambda, \lambda'; PS) \equiv \frac{\left| \sum_{\lambda_Z, \lambda_{Z'}} (M_{ZZ} + M_{AC})\, M_{Zf\bar{f}}\, M_{Z'f'\bar{f}'} \right|^2}{\left| \sum_{\lambda_Z, \lambda_{Z'}} M_{ZZ}\, M_{Zf\bar{f}}\, M_{Z'f'\bar{f}'} \right|^2} \tag{12}$$

The weight $W'^{ZZ}(\sigma, \lambda, \lambda'; PS)$ depends on the helicities of the initial electron (σ) and of the final fermions (λ,λ'). It also depends on the kinematic variables defining the phase space (PS). For convenience we choose the following set:

- The invariant masses of the $f\bar{f}$ and $f'\bar{f}'$ systems: M_Z, $M_{Z'}$.

- The polar and azimuthal angles of the $f\bar{f}$ system : θ_Z, ϕ_Z.
- The polar and azimuthal angles of the fermion f after a Lorentz boost to the rest frame of the $f\bar{f}$ system: θ_f, ϕ_f.
- The polar and azimuthal angles of the fermion f' after a Lorentz boost to the rest frame of the $f'\bar{f}'$ system: $\theta_{f'}$, $\phi_{f'}$.

The previous result can be extended to take into account other non-resonant diagrams like $e^+e^- \to Z\gamma^* \to f\bar{f}f'\bar{f}'$ and $e^+e^- \to \gamma^*\gamma^* \to f\bar{f}f'\bar{f}'$. The final weight is:

$$W^{VV}(\sigma,\lambda,\lambda';PS) \equiv \left| 1 + \frac{\mathcal{D}_Z(q^2)\mathcal{D}_{Z'}(q'^2) \sum_{\lambda_Z,\lambda_{Z'}} M_{AC}\, M_{Zf\bar{f}}\, M_{Z'f'\bar{f}'}}{\sum_{V_o,V'_o} \mathcal{D}_{V_o}(q^2)\mathcal{D}_{V'_o}(q'^2) \sum_{\lambda_{V_o},\lambda_{V'_o}} M_{V_oV'_o}\, M_{V_of\bar{f}}\, M_{V'_of'\bar{f}'}} \right|^2 \tag{13}$$

where a sum on all intermediate $V_o \in \{Z, \gamma^*\}$ is assumed. The propagator factors $\mathcal{D}_{V_o}$ are defined as follows in terms of the invariant mass of the fermion pair, q^2:

$$\mathcal{D}_Z(q^2) = \frac{1}{q^2 - m_Z^2 + i\,\Gamma_Z\, q^2/m_Z} \tag{14}$$

$$\mathcal{D}_\gamma(q^2) = \frac{1}{q^2} \tag{15}$$

where the imaginary component takes into account the energy dependence of the Z width around the resonance. The expressions for $M_{Z\gamma^*}$, $M_{\gamma^*\gamma^*}$, $M_{\gamma^* f\bar{f}}$ are obtained by the same method used for M_{ZZ} and $M_{Zf\bar{f}}$. Explicitly, they can be obtained by substituting Z by γ^* where necessary:

$$\epsilon_Z(\lambda_Z) \to \epsilon_{\gamma^*}(\lambda_\gamma) \tag{16}$$

$$M_Z \to M_{\gamma^*} \tag{17}$$

$$g_+^{Zf\bar{f}} \to g_+^{\gamma f\bar{f}} \tag{18}$$

$$g_-^{Zf\bar{f}} \to g_-^{\gamma f\bar{f}} \tag{19}$$

Weights according to $W^{VV}(\sigma,\lambda,\lambda';PS)$ have been implemented in a FORTRAN program. The approach is well suited for events generated with the PYTHIA $e^+e^- \to Z/\gamma^*\, Z/\gamma^* \to f\bar{f}f'\bar{f}'$ generator [4]. This implementation will be then identified as "PYTHIA approach". Several checks have been done in order to make sure that the calculations are correct. There is also agreement with the results obtained in [5] and in [6].

After reweighting, distributions according to given values of the anomalous couplings f_4^V, f_5^V are obtained . Detector effects are correctly taken into account if events are reweighted at generator level.

5 Initial state radiation effects

There are several references providing valuable information on the $e^+e^- \to ZZ$ process. A specific SM generator for $e^+e^- \to Z/\gamma^*\, Z/\gamma^*\, (\gamma) \to f\bar{f}f'\bar{f}'(\gamma)$ without anomalous couplings exists in

PYTHIA [4]. The calculation reported in the previous section is well suited for this MC generator, but initial state radiation effects (ISR) need to be taken into account. We assume that the differential cross section can be expressed as follows:

$$\frac{d\sigma(s)}{d(\text{Phase Space})} = \int ds' R(s,s') \frac{d\sigma(s')}{d(\text{Phase Space}')} \tag{20}$$

where $\sigma(s')$ is the (undressed) cross section evaluated at a scale s', and $\sigma(s)$ is the cross section after inclusion of ISR effects. The radiator factor $R(s,s')$ is a "universal" radiator, that is, independent of specific details of the matrix element. With this assumption ISR effects are accounted for by evaluating the matrix element in the center-of-mass system of the four fermions, at the corresponding scale s'.

In reference [5] a specific $e^+e^- \to ZZ(\gamma) \to f\bar{f}f'\bar{f}'(\gamma)$ generator for anomalous coupling studies is presented. It takes into account ISR effects with the YFS approach [7] up to $\mathcal{O}(\alpha^2)$ leading-log. It has some limitations, like the absence of conversion diagrams mediated by virtual photons.

The Standard Model cross section ($f_4^V = f_5^V = 0$) from [5] shows agreement at the percent level with the one determined in [8]. In the latter reference, it is shown that all significant radiation effects come from "universal" radiator factors. This implies that an approach based on equation 20 is justified in terms of the required precision.

6 The complete $e^+e^- \to f\bar{f}f'\bar{f}'$ process

Additional non-resonant diagrams are taken into account in SM programs for general four-fermion production, like EXCALIBUR [9]. Under a reasonable set of kinematic cuts, the relative influence of those diagrams can be reduced, but not totally suppressed. This is due to the low cross section for resonant ZZ production. Typical examples are those involving charged currents (relevant in $e^+e^- \to \nu_e\bar{\nu}_e f\bar{f}$, $e^+e^- \to u\bar{d}d\bar{u}$, ...) or multiperipheral effects in $e^+e^- \to e^+e^-f\bar{f}$. In addition, care must be taken for identical fermions (Fermi correlations in $e^+e^- \to f\bar{f}f\bar{f}$).

In order to avoid all these problems, the EXCALIBUR program has been extended. All matrix elements from conversion diagrams with two virtual Z particles $M_{ZZ}^{EXC}(\sigma,\lambda,\lambda';PS)$ are modified in the following way:

$$\Delta^{ZZ}(\sigma,\lambda,\lambda';PS) \equiv \frac{\sum_{\lambda_Z,\lambda_{Z'}} M_{AC}\, M_{Zf\bar{f}}\, M_{Z'f'\bar{f}'}}{\sum_{\lambda_Z,\lambda_{Z'}} M_{ZZ}\, M_{Zf\bar{f}}\, M_{Z'f'\bar{f}'}} \tag{21}$$

$$M_{ZZ}^{EXC}(\sigma,\lambda,\lambda';PS) \to M_{ZZ}^{EXC}(\sigma,\lambda,\lambda';PS)\,\left(1+\Delta^{ZZ}(\sigma,\lambda,\lambda';PS)\right) \tag{22}$$

where M_{ZZ}, M_{AC}, $M_{Zf\bar{f}}$ and $M_{Z'f'\bar{f}'}$ are the same terms defined in the PYTHIA approach. This method will be referred to as the "EXCALIBUR approach" in the following. More detailed studies are reported in the next section.

7 Checks of the Implementation

The cross sections for the different four-fermion channels taking into account all the Standard Model diagrams (EXCALIBUR) and taking into account only the neutral conversion diagrams are shown in

Figure 7. These cross sections are computed inside the cuts for signal definition: the invariant masses of the two fermion-antifermion pairs must be in the range 70 GeV-105 GeV; in the final states with electrons, these electrons must verify $|\cos\theta_e| < 0.95$ and in the final states with WW contributions, the invariant masses of the fermion pairs susceptible to come from W decay must be outside the range 75 GeV-85 GeV. Channels involving electron or electronic neutrino pairs in the final state have a non-negligible contribution coming from non-conversion diagrams. Also final states with fermions from the same isospin doublet ((ℓ, ν_ℓ),(u,d),(c,s)) show a non-negligible charged current contribution. Therefore the full set of diagrams should be taken into account for a correct analysis of the $e^+e^- \to ZZ$ experimental signal.

The second check in the calculation ensures that the results obtained from EXCALIBUR approach using only the neutral conversion diagrams are consistent with the results coming from the PYTHIA approach.The comparison is twofold. First, the Standard Model squared matrix elements are compared. Second, the effects of the anomalous couplings are also compared.

For the Standard Model matrix elements, the comparison can be seen in Figure 8. The squared matrix element computed using EXCALIBUR and the difference between EXCALIBUR and the PYTHIA-like determination are shown for three type of processes. The first one contains all the channels. The second one contains those diagrams in which there are no correlations between fermions in the final state ("Case 1"). There is perfect agreement between both approaches in this case. The last comparison is devoted to those channels in which correlations between fermions are important, namely, when there are two fermions of the same flavour in the final state ("Case 2"). EXCALIBUR takes into account the effect, whereas no effort has been done to include these correlations in the PYTHIA approach. The discrepancy is seen as a tail in the distribution.

To compare the implementations in the presence of anomalous couplings, the Standard Model distributions are reweighted according to the procedures described in previous sections. The difference between the weights assigned in each calculation is shown in Figures 9- 12. There is again a discrepancy when there are fermion correlations in the final state, but smaller than for the matrix elements. The reason must be found in the fact that the discrepancy factorizes in a similar way both for SM and anomalous coupling terms.

Finally, the last check evaluates the influence of the non-conversion diagrams when anomalous couplings are not zero. The averages of the reweighting factors for EXCALIBUR with only neutral conversion diagrams and EXCALIBUR with all the diagrams are compared in tables 1- 4, for the set of cuts defining the ZZ resonant region. The differences are typically below 10%, but can not be neglected.

$f_4^Z = 1.$	EXC CD	EXC ALL
$q\bar{q}q\bar{q}$	1.128	1.123
$q\bar{q}\nu\bar{\nu}$	1.131	1.150
$q\bar{q}l\bar{l}$	1.105	1.091
$l\bar{l}\nu\bar{\nu}$	1.101	1.082
$l\bar{l}l\bar{l}$	1.128	1.054
$\nu\bar{\nu}\nu\bar{\nu}$	1.084	1.170

Table 1: Average reweighting factors when $f_4^Z = 1$. Excalibur with only neutral conversion diagrams, compared to Excalibur with all Feynman diagrams.

$f_5^Z = 1.$	EXC CD	EXC ALL
$q\bar{q}q\bar{q}$	1.023	1.022
$q\bar{q}\nu\bar{\nu}$	1.019	1.024
$q\bar{q}l\bar{l}$	1.013	1.006
$l\bar{l}\nu\bar{\nu}$	1.025	1.013
$l\bar{l}l\bar{l}$	1.024	1.007
$\nu\bar{\nu}\nu\bar{\nu}$	1.022	1.036

Table 2: Average reweighting factors when $f_5^Z = 1$. Excalibur with only neutral conversion diagrams, compared to Excalibur with all Feynman diagrams.

$f_4^\gamma = 1.$	EXC CD	EXC ALL
$q\bar{q}q\bar{q}$	1.350	1.336
$q\bar{q}\nu\bar{\nu}$	1.339	1.385
$q\bar{q}l\bar{l}$	1.273	1.235
$l\bar{l}\nu\bar{\nu}$	1.218	1.181
$l\bar{l}l\bar{l}$	1.380	1.161
$\nu\bar{\nu}\nu\bar{\nu}$	1.254	1.463

Table 3: Average reweighting factors when $f_4^\gamma = 1$. Excalibur with only neutral conversion diagrams, compared to Excalibur with all Feynman diagrams.

$f_5^\gamma = 1.$	EXC CD	EXC ALL
$q\bar{q}q\bar{q}$	1.041	1.041
$q\bar{q}\nu\bar{\nu}$	1.047	1.050
$q\bar{q}l\bar{l}$	1.032	1.026
$l\bar{l}\nu\bar{\nu}$	1.031	1.004
$l\bar{l}l\bar{l}$	1.033	1.019
$\nu\bar{\nu}\nu\bar{\nu}$	1.071	1.082

Table 4: Average reweighting factors when $f_5^\gamma = 1$. Excalibur with only neutral conversion diagrams, compared to Excalibur with all Feynman diagrams.

8 Measurement of ZZZ and ZZγ anomalous couplings

To determine the values of the anomalous couplings from the data, the histogram of the most relevant variable for each four-fermion channel may be used. The following binned likelihood function is then maximized:

$$\log(\mathcal{L}) = \sum_{j=1}^{N_{bin}} \left[N_{data}(j) \log N_{expected}(j; f_i^V) - N_{expected}(j; f_i^V) \right] \tag{23}$$

The expected number of events is computed as: $N_{expected}(j; f_i^V) = N_{signal}(j; f_i^V) + N_{background}(j)$. The background contribution does not depend on the anomalous couplings. The signal contribution includes all four-fermion final states compatible with the exchange of two Z bosons. It is computed reweighting the Standard Model distributions with the EXCALIBUR approach and taking into account the f_i^V values of the anomalous couplings.

Good choices for discriminating variables are: invariant masses of the lepton pairs in leptonic decays, neural-net outputs for hadronic decays and optimal observables for all channels. This method is currently being applied in the analysis of $e^+e^- \to f\bar{f}f'\bar{f}'$ final states by the L3 Collaboration [1].

9 Acknowledgements

We would like to thank J. Biebel and A. Felbrich for useful discussions and cross-checks. We are also grateful to R. Pittau for providing his last version of the EXCALIBUR program for L3. We specially thank the help, positive criticism and support from our L3-ZZ collaborators during this time.

References

[1] L3 Collaboration, M. Acciarri *et al.*, L3 Preprint 169, Submitted to Phys. Lett. B (December 1998).

[2] K. Hagiwara *et al.*, Nucl. Phys. **B 282** (1987) 253–307.

[3] K. Hagiwara, D. Zeppenfeld, Nucl. Phys. **B 274** (1987) 1.

[4] T. Sjöstrand, CERN–TH/7112/93 (1993), revised August 1995;
T. Sjöstrand, Comp. Phys. Comm. **82** (1994) 74.

[5] S. Jadach, W. Placzek, B.F.L. Ward, Phys. Rev. **D 56** (1997) 6039.

[6] J. Biebel, DESY 98-163;
A. Felbrich, private communication.

[7] D.R. Yennie, S. Frautschi, H. Suura, Ann. Phys. **13** (1961) 379.

[8] D. Bardin, D. Lehner, T. Riemann, Nucl. Phys. **B 477** (1996) 27.

[9] F.A. Berends, R. Kleiss and R. Pittau, Nucl. Phys. **B 424** (1994) 308; Nucl. Phys. **B 426** (1994) 344; Nucl. Phys. (Proc. Suppl.) **B 37** (1994) 163;
R. Kleiss and R. Pittau, Comp. Phys. Comm. **83** (1994) 141;
R. Pittau, Phys. Lett. **B 335** (1994) 490.

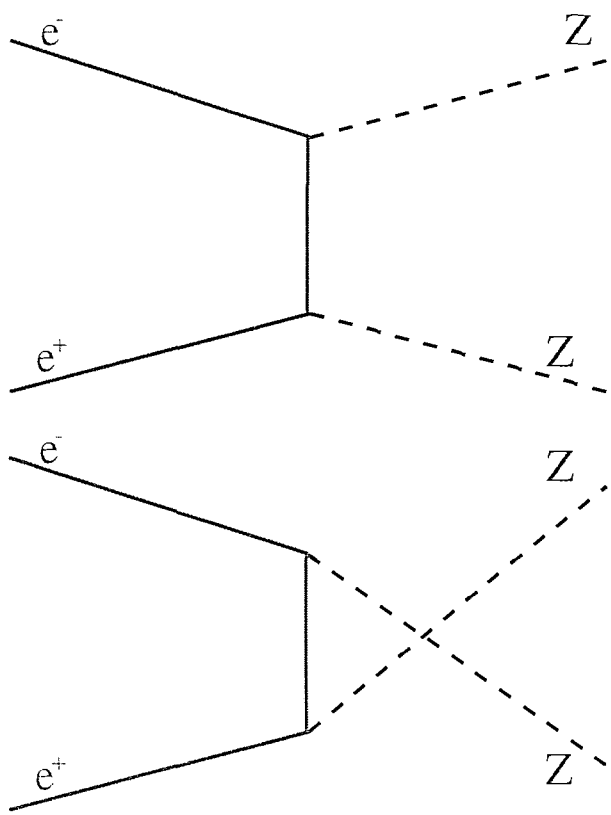

Figure 1: Diagrams contributing at first order to the Standard Model process $e^+e^- \to ZZ$.

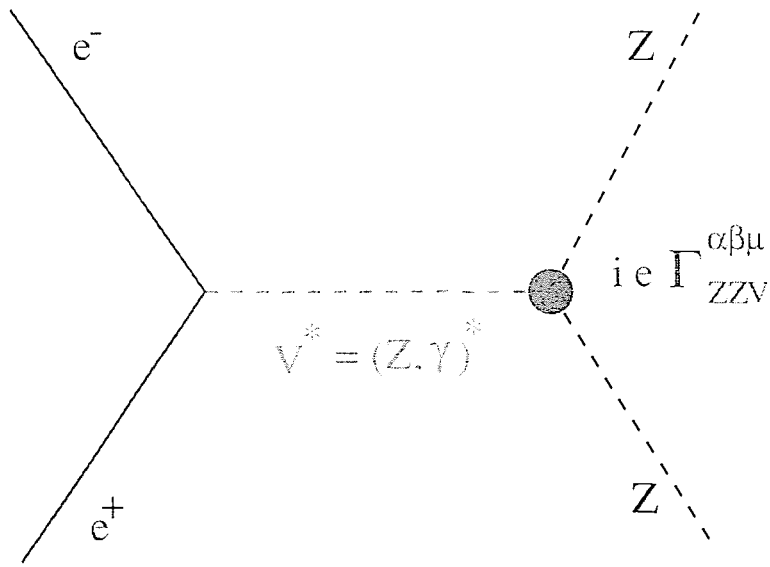

Figure 2: Diagram with anomalous $ZZ\gamma$ and ZZZ couplings contributing to the process $e^+e^- \to ZZ$.

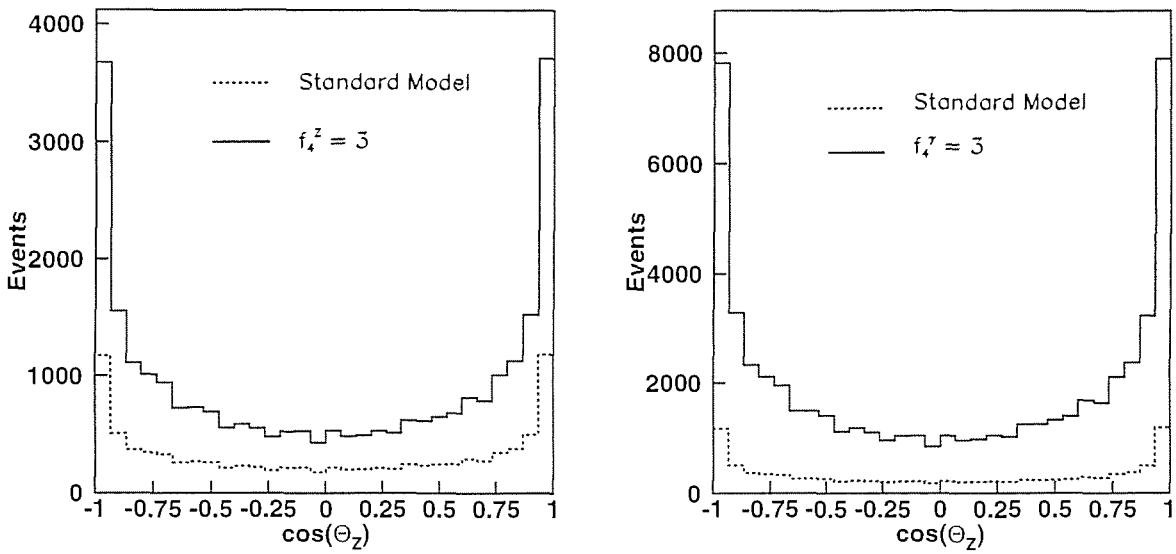

Figure 3: Effect of CP-violating non-standard couplings in the $e^+e^- \rightarrow ZZ$ process at $\sqrt{s} = 190$ GeV. A collision in the e^+e^- center-of-mass system is assumed. The angle θ_Z is the polar angle of one of the Z bosons.

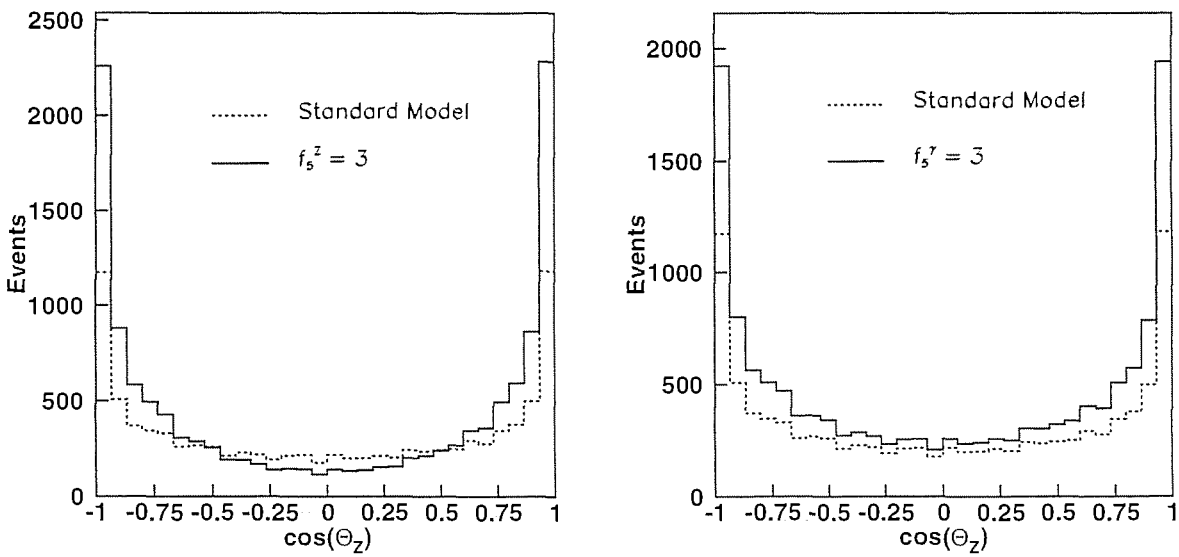

Figure 4: Effect of P-violating non-standard couplings in the $e^+e^- \rightarrow ZZ$ process at $\sqrt{s} = 190$ GeV. A collision in the e^+e^- center-of-mass system is assumed. The angle θ_Z is the polar angle of one of the Z bosons.

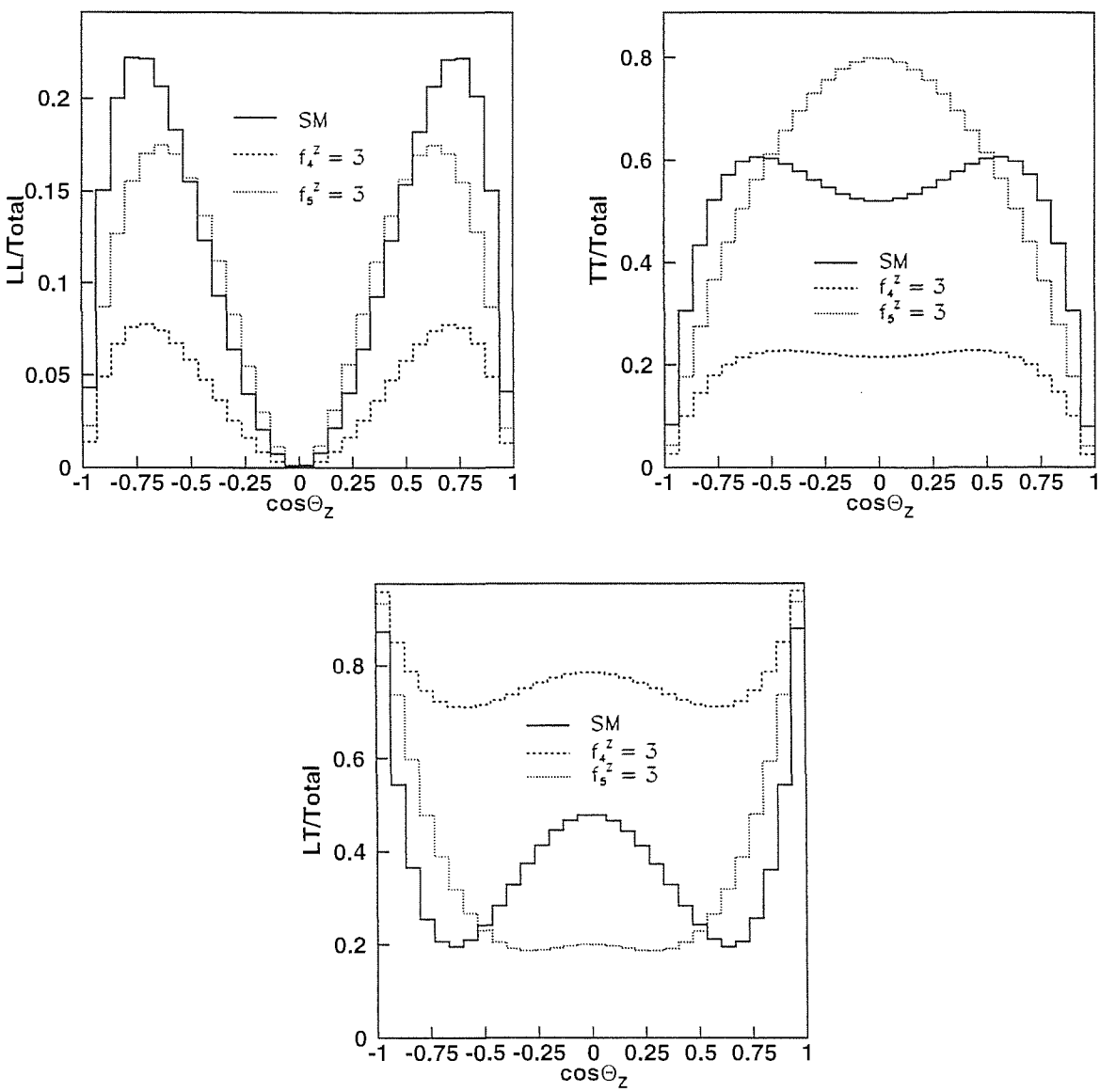

Figure 5: Proportion of events in which both Z are longitudinally polarized (top left), both Z are polarized transversely (top right) or one is longitudinally and the other is transversely polarized (bottom) in a $e^+e^- \to ZZ$ process at $\sqrt{s} = 190$ GeV. Predictions for SM (continuous line) and anomalous ZZZ couplings (dashed lines) are shown. A collision in the e^+e^- center-of-mass system is assumed. The angle θ_Z is the polar angle of one of the Z bosons.

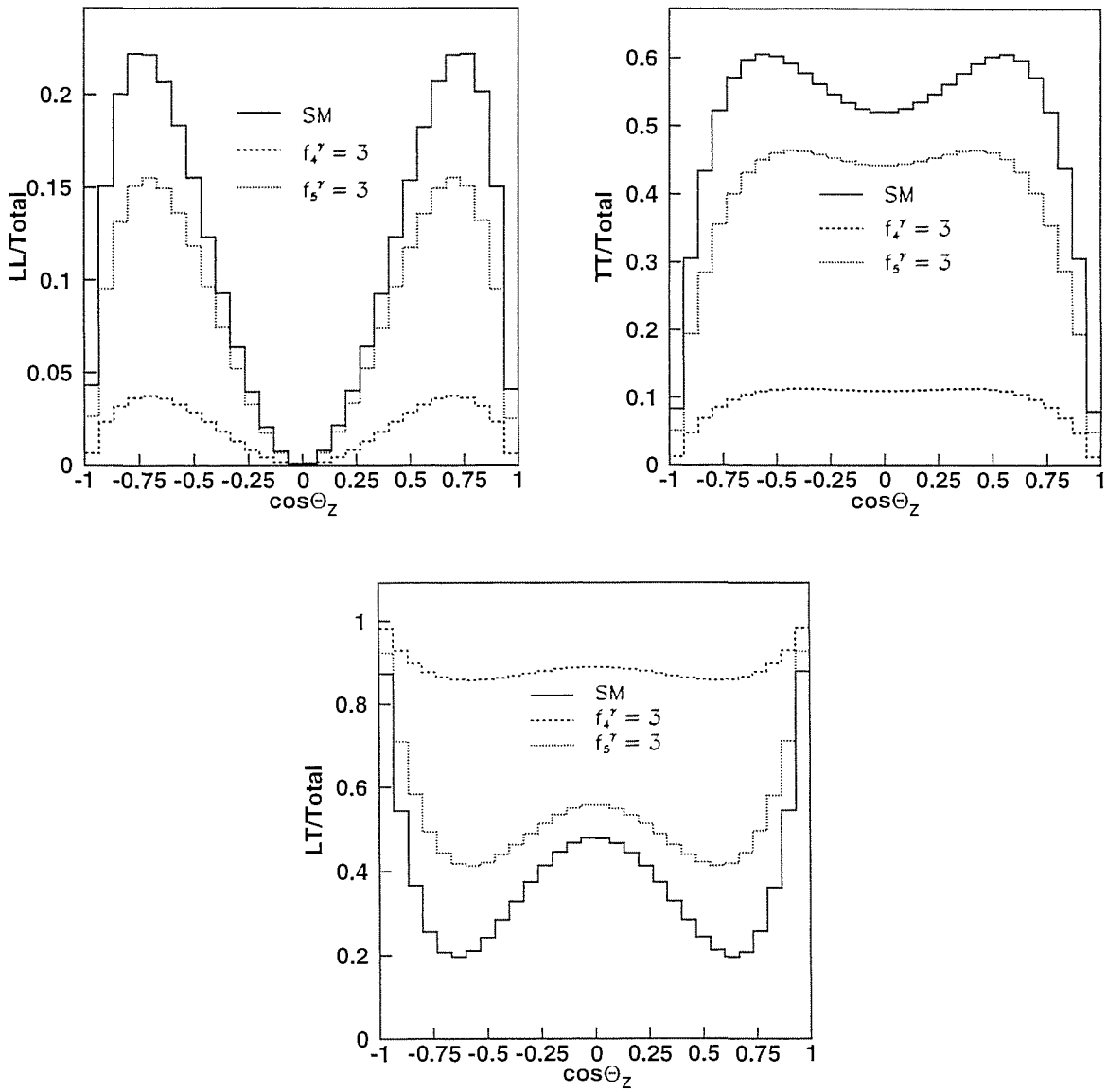

Figure 6: Proportion of events in which both Z are longitudinally polarized (top left), both Z are polarized transversely (top right) or one is longitudinally and the other is transversely polarized (bottom) in a $e^+e^- \to ZZ$ process at $\sqrt{s} = 190$ GeV. Predictions for SM (continuous line) and anomalous $ZZ\gamma$ couplings (dashed lines) are shown. A collision in the e^+e^- center-of-mass system is assumed. The angle θ_Z is the polar angle of one of the Z bosons.

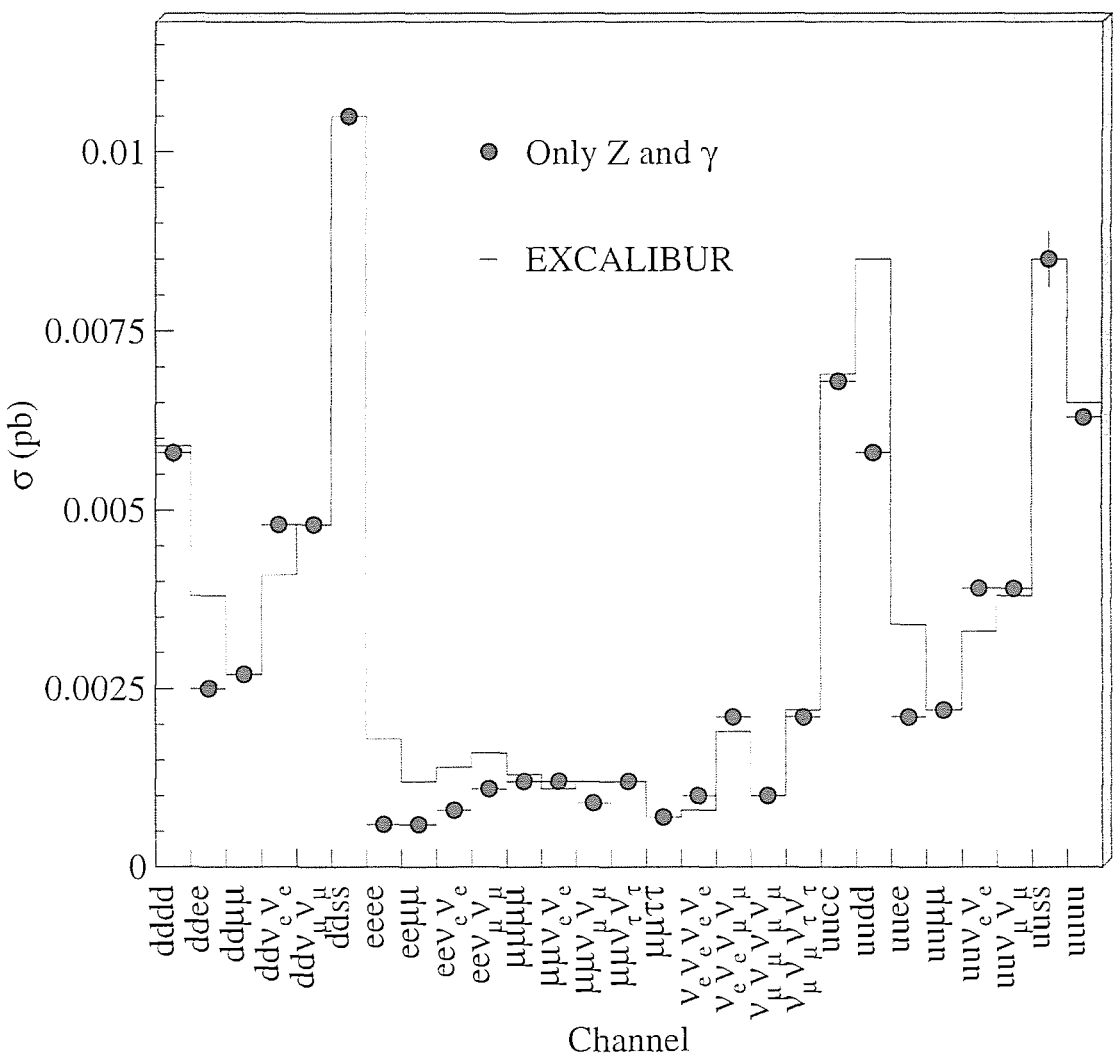

Figure 7: Cross sections for the different four-fermion channels taking into account all the diagrams (histogram) and only the neutral conversion ones (dots). Some cuts (described in the text) have been applied in order to enhance the ZZ resonant contribution. Other diagrams are important when electrons, electronic neutrinos or fermions from the same isospin doublet are present in the final state.

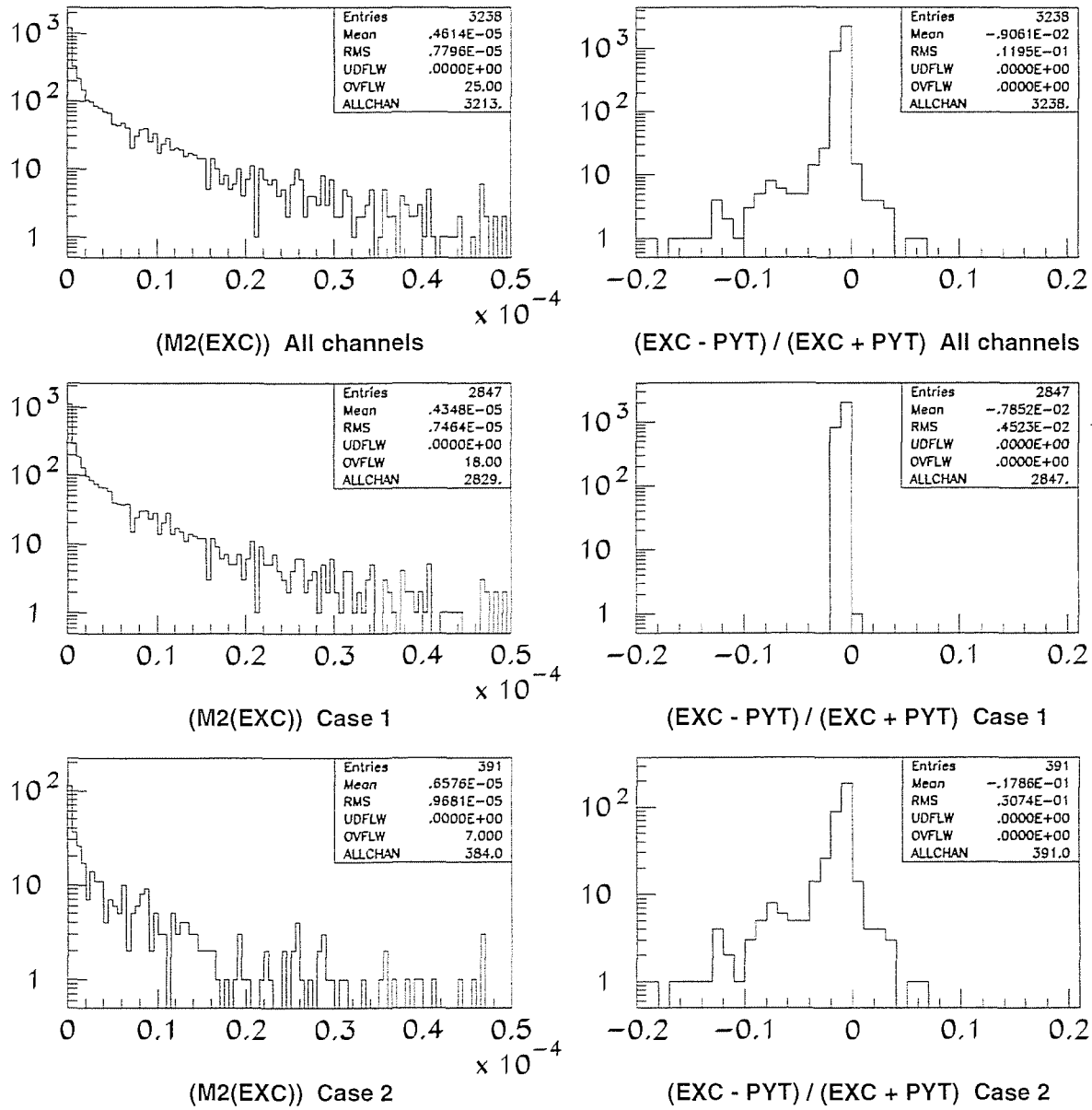

Figure 8: Squared matrix element from EXCALIBUR (left column) and comparison between EXCALIBUR (EXC) and PYTHIA-like (PYT) calculations for the squared matrix element (right column). Only neutral conversion diagrams are taken into account. The first row uses all the channels. The second row is done with those channels with no fermion correlations in the final state. The third row comes from the channels with fermion correlations in the final state. The effect of Fermi correlations (no effort has been done to include them in our PYTHIA-like approach) is visible as a tail in the distribution.

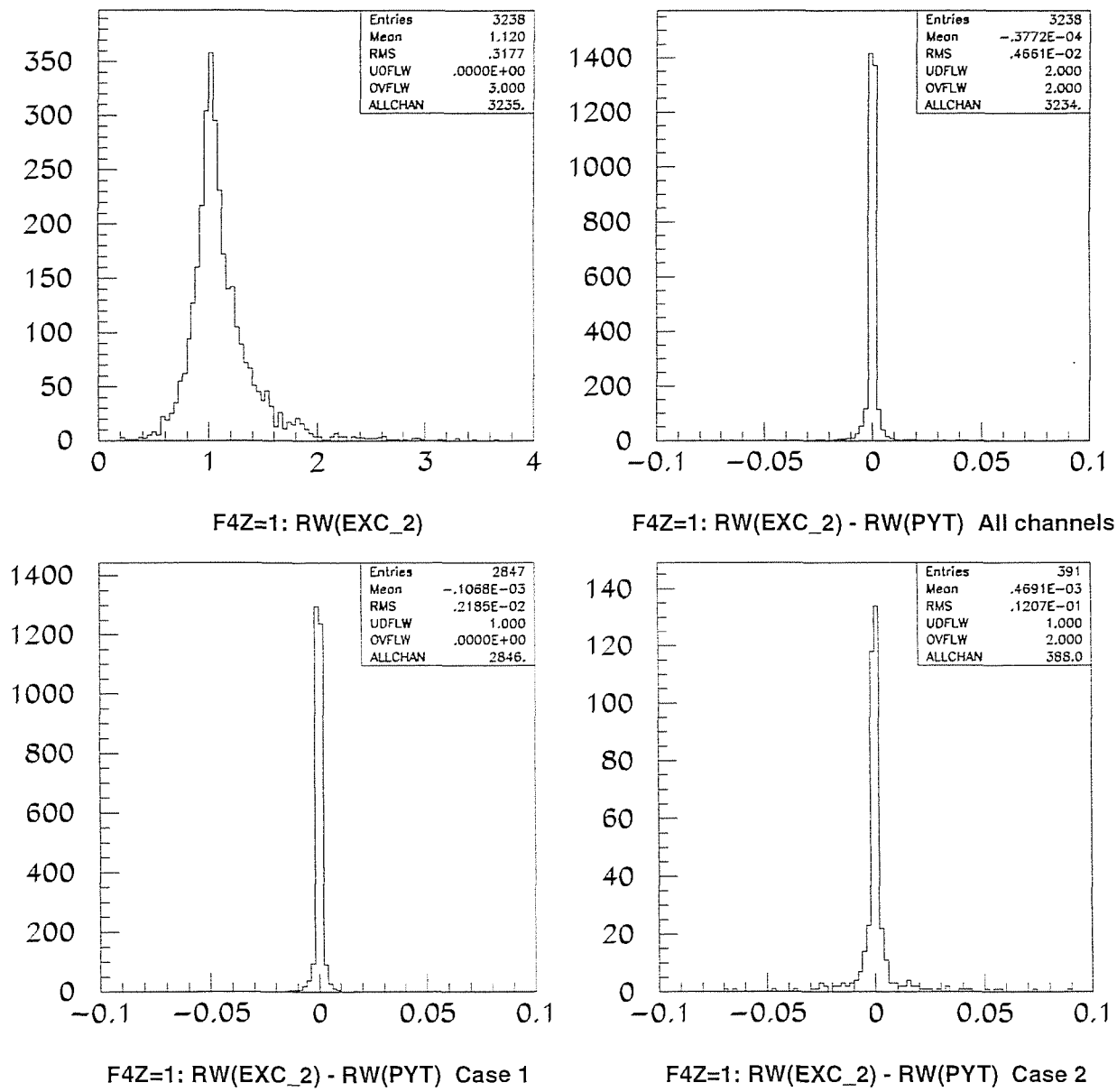

Figure 9: Reweighting factor obtained with EXCALIBUR (upper left) for $f_4^Z = 1$. In the upper right the difference in the reweighting factor between the EXCALIBUR-like (EXC_2) and the PYTHIA-like (PYT) approaches is shown. Only neutral conversion diagrams are taking into account. In the lower part, the same difference is shown for the final states without (left) and with (right) fermion correlations in the final state.

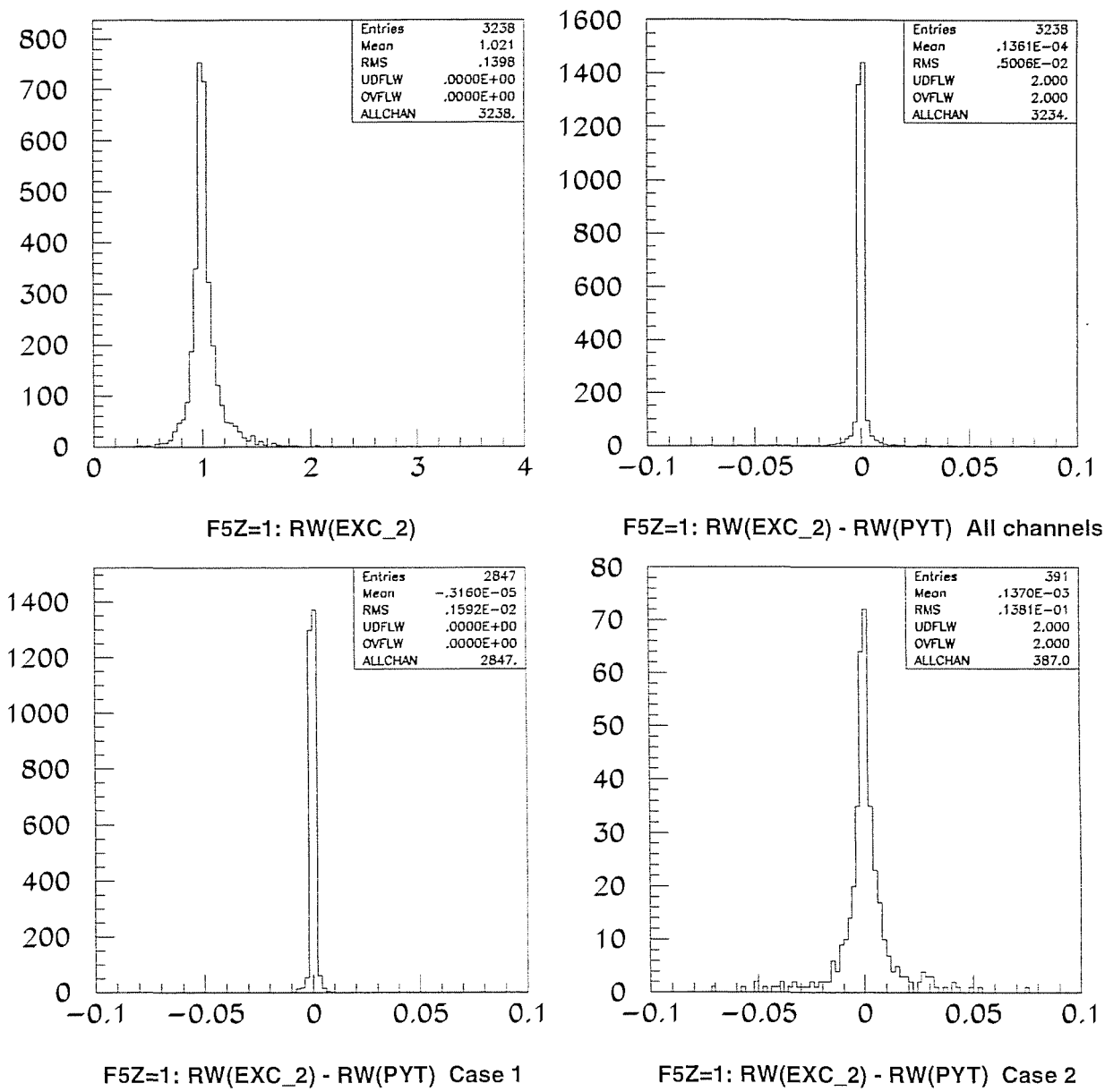

Figure 10: The same that for Fig. 9 but for $f_5^Z = 1$.

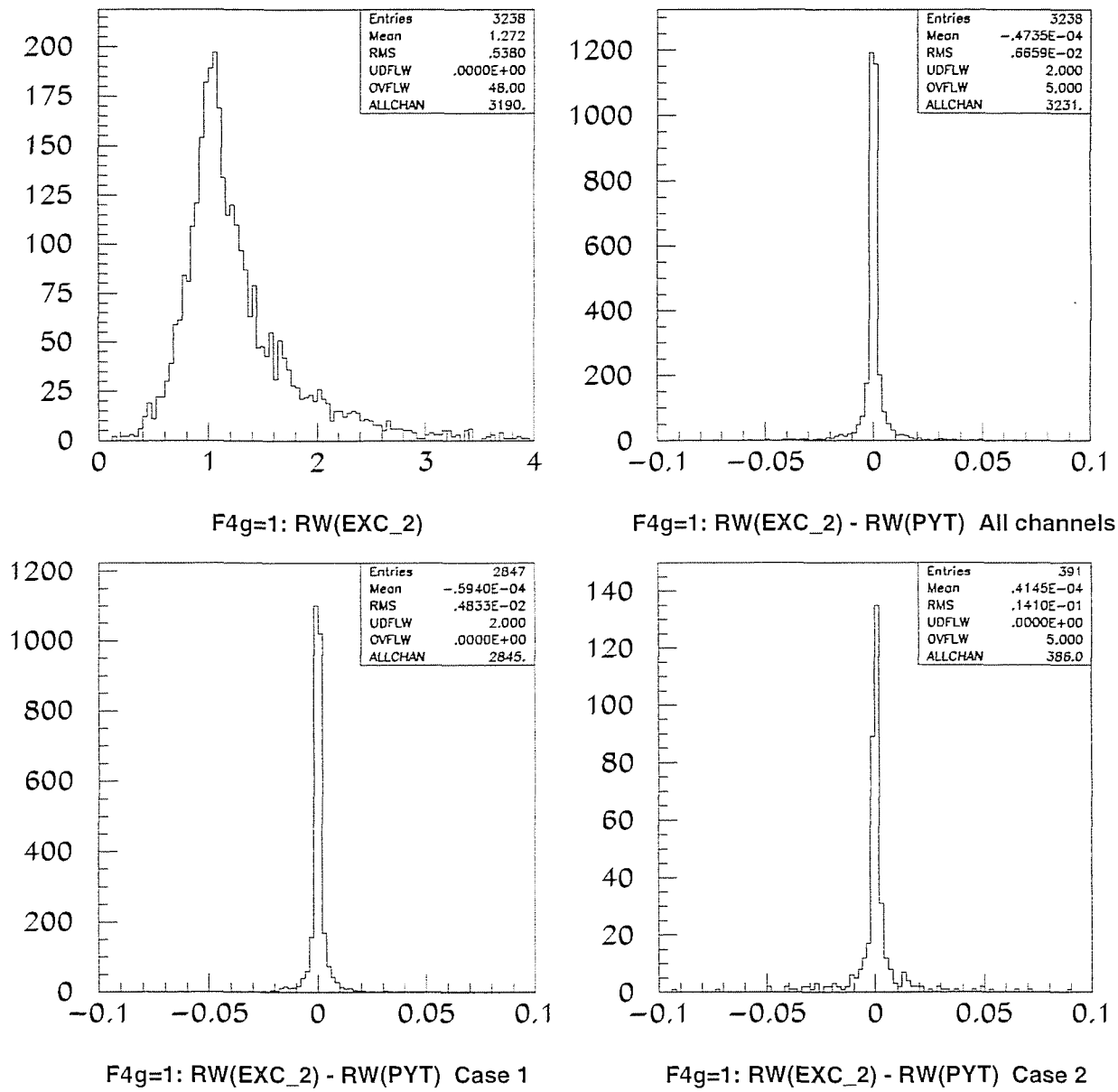

Figure 11: The same that for Fig. 9 but for $f_4^\gamma = 1$.

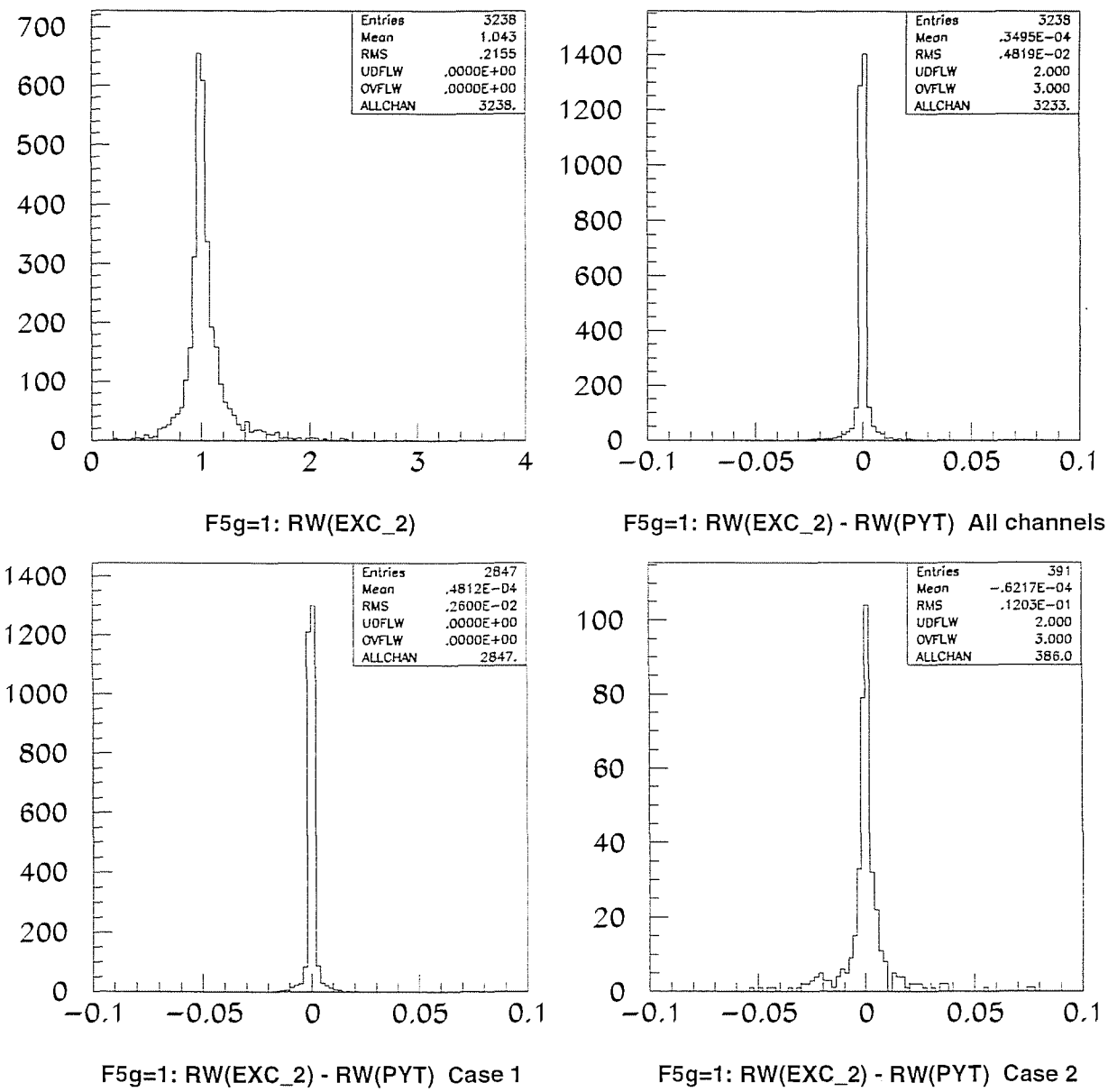

Figure 12: The same that for Fig. 9 but for $f_5^\gamma = 1$.